Unphysical damping of turbulence when passing a numerically captured shock

By J. Larsson

1. Motivation and objectives

The presence of shock waves is an important feature of high-speed fluid flows. At physically relevant Mach- and Reynolds-numbers the shock thickness is vanishingly small; therefore the only realistic computational approach is to either treat the shock as an interface ("shock-fitting") or to use numerics that smear the shock over a few grid points while predicting the correct shock jumps ("shock-capturing"). The main advantage of the shock-capturing class of methods is the ability to handle shocks of arbitrary topology.

The present work is focused on direct numerical or large eddy simulation (DNS and LES, respectively) of flows involving both shocks and turbulence. In such high-fidelity calculations, it is vital to be aware of and estimate all possible sources of error. Consider the canonical case of isotropic turbulence passing through a normal shock, for which some sample results are shown in Fig. 1. The figure shows the streamwise evolution of the transverse Reynolds stress R_{22} before and after the shock. The shock oscillates around its mean position in response to the turbulence; the extent of this motion is shown as the "width" in the figure. The instantaneous thickness of the shock, however, is about 3 grid points wide and much smaller than the "width" shown in the figure. The figure illustrates several different sources of error due to numerical dissipation and insufficient grid resolution:

(a) Upstream of the shock, the dissipative method yields too fast decay of the isotropic turbulence. This error can be eliminated by use of a non-dissipative method (dashed line in the figure), and has been well documented in the literature (cf. Mittal & Moin 1997; Larsson *et al.* 2007).

(b) Downstream of the shock, one must (in the case of DNS) resolve the viscous dissipation; this occurs at smaller length scales than upstream (Larsson 2008).

(c) At the shock, all shock-capturing methods necessarily must introduce numerical dissipation. However, the figure shows that the amplification of R_{22} across the shock is underpredicted on the coarse grid (compare the solid and dashed lines). This error affects both DNS and LES, and has not been analyzed in the existing literature (to the author's knowledge). It is, therefore, the topic of the present work.

There is a wide array of shock-capturing methods in the literature. These methods may be high-order accurate when applied to smooth problems, but they must necessarily be first-order accurate in the L_1 norm when applied to a shock (or any discontinuity). This is easily understood by the facts that 1) the shock will occupy a constant number of grid points regardless of the grid spacing, and 2) there will always be a point-wise error proportional to the shock-jump due to the smearing.

Although it is clear that shock-capturing methods are first-order accurate in the L_1 norm, it is not clear that this definition of the error is the most relevant in practice. Consider the case of turbulence interacting with (i.e., passing through) a shock wave. One key feature of shock/turbulence interaction is the amplification of Reynolds stresses

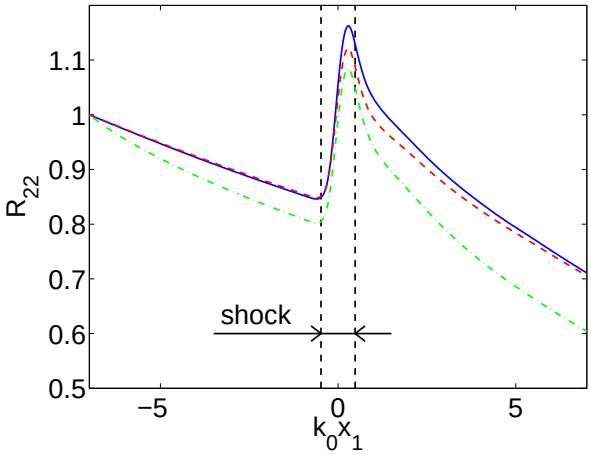

FIGURE 1. Illustration of different sources of error in shock/turbulence interaction: transverse Reynolds stress $R_{22} = \widetilde{u_2'' u_2''}$ from DNS at mean Mach number 1.5 and Reynolds number $Re_\lambda \approx 40$. The solid line is the converged result on a grid with $(k_0 h_1, k_0 h_{2,3}) = (2\pi/192, 2\pi/96)$ using a method that eliminates numerical dissipation away from the shock. The dashed line uses the same method, but with a coarse grid with $(k_0 h_1, k_0 h_{2,3}) = (2\pi/64, 2\pi/32)$. The dash-dotted line uses a dissipative 7th-order WENO scheme everywhere on the same coarse grid. The curves have been normalized by their values at the inlet to facilitate comparison, and the dashed vertical lines show the extent of the unsteady shock motion.

and vorticity. These (and other) quantities are insensitive to phase information; therefore the convergence of turbulence statistics is not necessarily a first-order process. In computations of shock/turbulence interactions, using either LES or DNS, one would want to design the grid such that the error in the post-shock turbulence statistics is less than some acceptable level. This can only be done a priori if the relationship between the shock-normal grid spacing, the numerical method, and the error in the post-shock turbulence statistics is known.

The objective of this work is to develop an approximate estimate to this relationship. A key consideration has been to strike a balance between analytical simplicity and application relevance, although this is not trivial. At the outset, the error estimate is required to be valid for broadband three-dimensional turbulence to ensure relevance to applied LES and DNS. To simplify the analysis, only isotropic upstream turbulence and normal shock waves are considered here. These are obvious limitations, but the general conclusions should be applicable to anisotropic turbulence and/or oblique shocks as well. In addition, rapid distortion theory (RDT) is used to approximate the turbulence-modification due to the shock, despite its well-known shortcomings in describing shock/turbulence interactions.

1.1. *Notation*

Subscripts will be used to denote both tensor indices and whether a point is upstream or downstream of the shock, with numbers and letters, respectively. For example, $k_{1,\mathrm{u}}$ is the streamwise (shock-normal) wavenumber upstream of the shock, whereas $u_{2,\mathrm{d}}$ is the transverse velocity downstream of the shock.

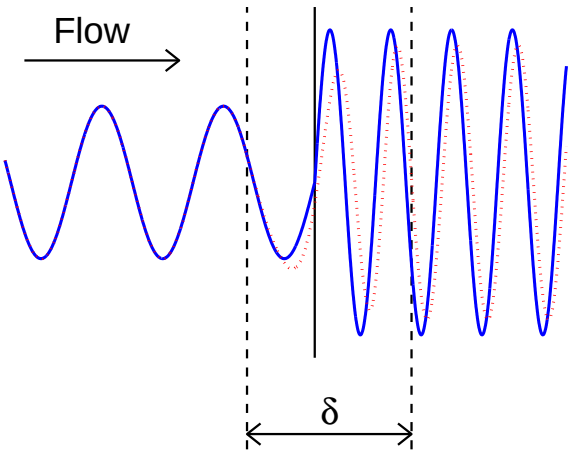

FIGURE 2. Sketch of idealized error mechanism in shock-capturing schemes. The solid line shows an incoming signal being modified by the infinitesimal shock (thin solid line) to a higher amplitude and shorter wavelength. The dotted line shows a signal affected by the shock-capturing dissipation (and dispersion) within the numerical shock thickness (δ), leading to both amplitude and phase errors behind the shock.

2. Error model

Shock-capturing schemes work by adding numerical diffusion that smears the shock over a few grid points, thereby allowing it to be captured by the numerical method. A simple balance of convective and viscous terms (in the Navier-Stokes equations) in a frame where the shock is stationary yields $\rho u_1 \Delta u_1/h \sim \rho\nu\Delta u_1/h^2$, where ρ is the density, Δu_1 is the jump in velocity at the shock, ν is the kinematic viscosity, and h is the grid spacing. This gives $\nu \sim u_1 h$, which shows that shock-capturing necessarily must introduce dissipation that depends linearly on the grid spacing, i.e., that is first-order accurate.

In the present work, the modification to an incoming signal u is idealized in two steps: 1) the exact modification due to the shock-compression, and 2) the error introduced when the signal is propagating through the "viscous" region around the shock. This scenario is sketched in Fig. 2, where δ denotes the narrow region where the shock-capturing numerics add significant numerical dissipation. The amount of dissipation in this region and its width δ depend on the shock-capturing method and possibly the Mach number of the shock. However, for all methods $\delta \sim h$. Within this idealization it is clear that the error in the post-shock variance of the signal is second order in the grid spacing: loosely speaking, the signal encounters a viscosity $\nu \propto h$ during a time $t \propto \delta \sim h$, which implies that the signal is damped by a factor $\propto h^2$. One purpose of this work is to verify this view of the shock-capturing error. One simple error metric is the relative error in the post-shock Reynolds stresses $R_{ij} = \widetilde{u_i'' u_j''}$, where $\tilde{\cdot}$ denotes a density-weighted (Favre) average and the double-prime $''$ denotes fluctuation around this average. The relative error in R_{ij} is defined as

$$\epsilon_{ij} = \frac{R_{ij}|_{h=0} - R_{ij}|_h}{R_{ij}|_{h=0}}, \tag{2.1}$$

where subscript $h = 0$ implies the exact or converged value of the average. The purpose of the following is to develop a simple model that predicts this error.

We first assume that the upstream turbulence is isotropic with zero density fluctuations, with a velocity field that satisfies the von Karman spectrum (cf. Pope 2000)

$$E(k) = 1.1185\,\frac{u^2}{k_0}\,\frac{(k/k_0)^2}{\left[(k/k_0)^2 + 5/6\right]^{11/6}}\,, \tag{2.2}$$

where the spectrum has been written on a form that gives peak energy at wavenumber k_0. To approximate LES, the spectrum is truncated at the cut-off wavenumber $k_{\max} = \pi/h$.

To get an expression for the error in the post-shock statistics, we need to approximate both the inviscid compression of the turbulence and the damping due to numerical dissipation. A simple approach is to use homogeneous rapid distortion theory (RDT) where the velocity fluctuations are assumed to be solenoidal. The most obvious flaw in RDT is the assumption of homogeneity, which is incorrect at the shock; a second flaw is that RDT neglects the generation of acoustic and entropy waves during the interaction.

Decomposing the velocity as $u_i = U_i + u_i'$, the mean compression is taken as $\partial_1 U_1 = -S$ and $\partial_j U_i = 0$ for $(i,j) \neq (1,1)$. With the assumption of solenoidal turbulence u_i', the RDT-system becomes (cf. Pope 2000)

$$\begin{aligned}
\partial_t \rho &= S\rho\,,\\
\partial_t u_i' &= -U_1 \partial_1 u_i' + S u_1' \delta_{i1} - \frac{\partial_i p'}{\rho} + \nu \partial_{jj}^2 u_i'\,,
\end{aligned}$$

where the viscous term in the Navier-Stokes equations has been kept for later use in modeling the shock-capturing dissipation. Following Pope (2000), this system is solved using a time-dependent wavenumber k_1 that satisfies $\partial_t k_1 = S k_1$. We also introduce the normalized time $\tau = St/\ln(r)$, where $r = \rho_{\mathrm{d}}/\rho_{\mathrm{u}}$ is the compression ratio of the shock. This yields

$$\frac{d\widehat{u}_i}{d\tau} = \ln(r)\left[\left(\delta_{i1} - 2\frac{k_1 k_i}{k^2}\right)\widehat{u}_1 - \frac{\nu k^2}{S}\,\widehat{u}_i\right]\,, \tag{2.3a}$$

$$k_1 = k_{1,\mathrm{u}}\, r^{\tau}\,, \tag{2.3b}$$

where δ_{ij} is the Kronecker delta and $\widehat{u}_i$ is the Fourier transform of the velocity. Note that this is to be integrated from $\tau = 0$ to 1.

We now seek to model the effect of the numerical shock-capturing dissipation in this framework. Any shock-capturing method necessarily reduces to first order at the shock; therefore the numerical viscosity should scale as $\nu \sim \Delta U_1 h \sim S h^2$. Since shock-capturing methods tend to capture shocks over a constant number of grid points, one might expect $\nu \approx C S h^2$ for some constant C that should depend on the numerical method but not on the shock compression ratio.

This expression for ν could be inserted into Eqn. (2.3a) directly, but this is not done here. The main flaw of RDT is the assumption of homogeneity. Observations from numerical experiments suggest that most of the numerical dissipation occurs on the downstream-side of the smeared shock. This is plausible, for two reasons: 1) the shock compresses the turbulence to higher wavenumbers (that are more affected by dissipation), and 2) the downstream convection velocity is lower, implying that the turbulence spends more time within the numerical shock thickness δ on the downstream side. This effect can be approximately accounted for in the homogeneous RDT by modeling the full viscous term

as

$$\frac{\nu k^2}{S}\,\widehat{u}_i \approx Ch^2 k_{\mathrm{d}}^2\,\widehat{u}_i\,,$$

i.e., by replacing (in the viscous term only) the time-dependent wavenumber $k^2 = k_j k_j$ by its downstream value $k_{\mathrm{d}}^2 = k_{1,\mathrm{u}}^2 r^2 + k_2^2 + k_3^2$. With this modeled shock-capturing dissipation, the final RDT-model of the numerical shock/turbulence interaction becomes

$$\begin{aligned} \frac{d\widehat{u}_i}{d\tau} &= \ln(r)\left[\left(\delta_{i1} - \frac{2\kappa_1\kappa_i}{\kappa^2}\right)\widehat{u}_1 - Ck_0^2h^2\kappa_{\mathrm{d}}^2\,\widehat{u}_i\right]\,, \\ \kappa_1 &= \kappa_{1,\mathrm{u}}\,r^{\tau}\,, \end{aligned} \tag{2.4}$$

where the non-dimensional wavenumber $\kappa_i = k_i/k_0$ has been introduced, with k_0 being a characteristic wavenumber of the upstream turbulence. It is taken as the wavenumber of peak energy in the present study, but could also be taken to correspond to the integral length scale or similar.

The RDT-model (2.4) is a function of the shock compression ratio r, the non-dimensional grid spacing k_0h, and the upstream energy spectrum $E(k)$ (through the initial condition). The constant C in the expression for the implied numerical dissipation is unknown and depends on the numerical method. For three-dimensional initial conditions the RDT-model can be solved numerically using any ODE-solver, but an analytical solution is possible for single-mode disturbances.

2.1. *Analytical solutions for single-mode disturbances*

We consider two idealized cases where the incoming disturbance consists of a single mode. When coupled with a numerical experiment, the analytical solution allows for the constant C to be determined. In addition, the analysis illuminates some features of the error introduced by the shock-capturing.

Consider first the single-mode disturbance given by $k_{1,\mathrm{u}} = k_0$, $\widehat{u}_{2,\mathrm{u}} \neq 0$, and $k_2, k_3, \widehat{u}_1, \widehat{u}_3$ all zero, i.e., a disturbance in the transverse velocity component. The RDT-model (2.4) for this case becomes

$$\frac{d\widehat{u}_2}{d\tau} = -C\ln(r)k_0^2h^2r^2\,\widehat{u}_2\,,$$

which can be solved analytically. Inserting the solution into the error definition (2.1) and expanding the exponential yields the predicted error as

$$\epsilon_{22,\ \mathrm{single-mode}} \approx 2C\ln(r)r^2k_0^2h^2\,. \tag{2.5}$$

Next consider a disturbance in the shock-normal velocity component, i.e., with $k_2 = k_0$, $\widehat{u}_{1,\mathrm{u}} \neq 0$, and $k_{1,\mathrm{u}}, k_3, \widehat{u}_2, \widehat{u}_3$ all zero. Again solving the RDT-model analytically and inserting the solution into the error definition yields the predicted error as

$$\epsilon_{11,\ \mathrm{single-mode}} \approx 2C\ln(r)k_0^2h^2\,. \tag{2.6}$$

For both transverse and normal disturbances, the RDT-model predicts that the error is second order in the grid spacing. This is consistent with the simple arguments given above. Interestingly, the model predicts different error-scalings with the strength of the shock r, with the error in the normal and transverse components scaling as $\ln(r)$ and $\ln(r)\,r^2$, respectively. The factor r^2 makes intuitive sense, since this corresponds to the increase in shock-normal wavenumber during the interaction with the shock. The RDT-model assumes solenoidal turbulence, thus zero streamwise wavenumber for the normal velocity disturbances; hence the factor r^2 is absent in $\epsilon_{11,\ \mathrm{single-mode}}$.

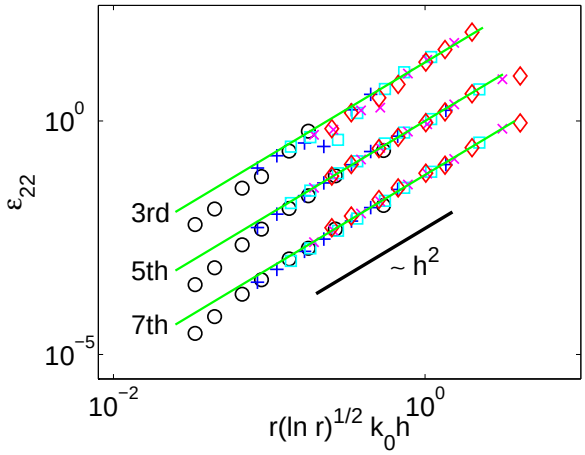

FIGURE 3. Error in Reynolds stress from numerical experiment of one-dimensional single-mode disturbance at 5 different Mach numbers corresponding to density jumps r of 1.5 (circles), 2.5 (plusses), 3.5 (squares), 4.5 (crosses), and 5.5 (diamonds). The predicted error from equation (2.5) is shown in solid lines, with the constant C chosen to best fit the results. Results from 7th-order WENO ($C = 0.035$), 5th-order WENO ($C = 0.050$, offset by factor 10), and 3rd-order WENO ($C = 0.090$, offset by factor 100).

3. Numerical experiment: single-mode transverse disturbance

A first verification of the predictions of the error model is done by computing a numerical experiment of a single-mode interaction. This is done only for the transverse incoming disturbance. The numerical experiment is set up with a stationary shock, and the post-shock Reynolds stress R_{22} is calculated by averaging over several periods in time. A range of mean Mach numbers are chosen to yield density jumps of r=1.5, 2.5, 3.5, 4.5, and 5.5. With gas constant $\gamma = 1.4$, this implies Mach numbers of $\approx$ 1.29, 1.89, 2.65, 3.87, and 7.42. At the inlet, the transverse velocity is set to $u_{2,\mathrm{u}} = 0.01\widetilde{u}_{1,\mathrm{u}} \cos(k_0 \widetilde{u}_{1,\mathrm{u}} t)$, i.e., a disturbance with wavenumber k_0 and 1% amplitude. The shock is located one wavelength from the inlet, and a sponge region is used to damp the solution before reaching the outlet boundary. The experiment is run using WENO schemes (cf. Jiang & Shu 1996) of 7th, 5th, and 3rd order accuracy with Roe flux-splitting. The computed errors are shown in Fig. 3. Also shown are the predicted error scalings from (2.5), with C chosen to best fit the results. The results show several things. First, the error is second order in the grid spacing, as expected. Secondly, the errors from the different Mach numbers collapse onto a single curve. Given the large range in Mach numbers, this suggests that the RDT-model correctly predicts this effect. Finally, as expected the effect of the numerical method shows up in the constant C. A fit to the numerical results yields

$$C = \begin{cases} 0.090 & , \quad 3\mathrm{rd-order\ WENO} \\ 0.050 & , \quad 5\mathrm{th-order\ WENO} \\ 0.035 & , \quad 7\mathrm{th-order\ WENO} \end{cases} .$$

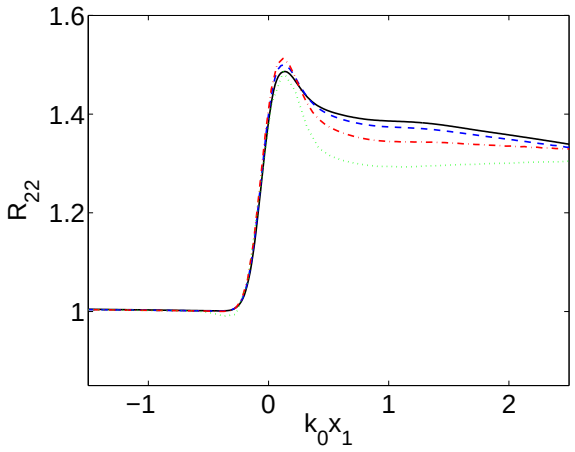

FIGURE 4. Convergence of transverse Reynolds stress $R_{22} = \widetilde{u_2'' u_2''}$ as the shock-normal grid spacing h_1 is refined, with $k_0 h_1$ of $2\pi/512$ (solid), $2\pi/256$ (dashed), $2\pi/128$ (dash-dotted), and $2\pi/64$ (dotted). Mean Mach number 1.87, Reynolds number $Re_\lambda \approx 200$, with transverse grid spacing $k_0 h_{2,3} = 2\pi/16$. The Reynolds stress is normalized by its value immediately upstream of the shock.

4. Numerical experiment: broadband isotropic turbulence

The next numerical experiment is the interaction between isotropic turbulence and a normal shock wave. The method by Ristorcelli & Blaisdell (1997) is used to generate isotropic turbulence with peak energy at wavenumber $k_0 = 4$, which is then allowed to decay in a periodic box of size $(2\pi)^3$ until it becomes fully developed. This developed turbulence is fed into the domain where it interacts with a normal shock. Immediately upstream of the shock, the Reynolds number based on the Taylor scale (cf. Pope 2000) is $Re_\lambda \approx 200$ and the mean Mach number is 1.87. The transverse grid spacing $h_{2,3}$ is held constant for all cases at $k_0 h_{2,3} = 2\pi/16$, or 16 points per wavelength of the most energetic mode. This is representative of LES, and much coarser than that required to resolve the viscous dissipation. The simulations are run without any subgrid model to truly represent underresolved LES, and to remove the (basically unknown) behavior of the subgrid model at the shock as a source of uncertainty. To minimize numerical dissipation, a 6th-order accurate central difference scheme is used away from the shock, whereas the 5th-order WENO scheme is used around the shock. Details of the numerical method can be found in Larsson (2008). Fig. 4 shows a sample of the convergence process. Note that the "width" of the averaged shock is entirely set by the unsteady shock-wrinkling; the instantaneous shock profiles are much steeper than these averaged profiles. It is clear that the turbulence is damped in the shock-region by the numerical dissipation, and that this yields significant errors in the post-shock Reynolds stress. For this case, a shock-normal grid spacing that is about 16 times finer than the transverse grid spacing is required to bring the error in the post-shock transverse Reynolds stress below 1%.

The error in the post-shock Reynolds stresses as defined by (2.1) is shown in Fig. 5, along with the predicted error from the RDT-model. First, it is clear that the errors in both the shock-normal and transverse components are second order in the grid spacing h_1 for sufficiently fine grids. Hence the idealized picture of the shock-capturing error given

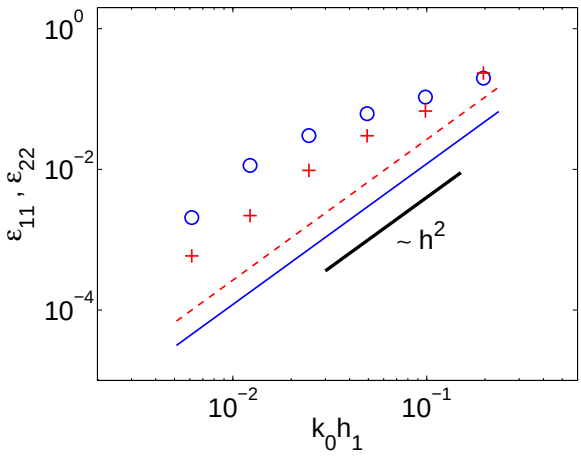

FIGURE 5. Error in the post-shock Reynolds stresses from numerical experiment of three-dimensional isotropic turbulence at Mach 1.87 with underresolved LES-like grid (symbols), compared with the predicted error from the RDT-model (lines). Shock-normal component ϵ_{11} (circles, solid line) and transverse component ϵ_{22} (plusses, dashed line).

above is valid even with broadband three-dimensional turbulence. In contrast to the single-mode experiment, the errors with three-dimensional turbulence are much larger than predicted by the RDT-model, especially in the shock-normal Reynolds stress. The reason for this discrepancy is that the RDT-model fails to take into account both the unsteady shock motion (which affects the amplification ratios) and the generation of sound waves by the shock/turbulence interaction (which primarily affects the shock-normal velocity field). Nevertheless, the RDT-model gives the correct scaling of the error and is therefore a useful tool for designing grids that minimize the error induced by the shock-capturing dissipation.

5. Summary and discussion

It is argued and verified that the error in the post-shock Reynolds stresses is second, not first, order in the shock-normal grid spacing when a shock-capturing numerical scheme is used. While not shown, this also holds for several other statistics, e.g., vorticity variances. An error model based on Rapid Distortion Theory (RDT) is proposed in the spirit of having a model that is simple yet applicable to three-dimensional turbulence. The RDT-model is shown to correctly predict the error scaling in both single-mode and broadband numerical experiments, and to correctly predict how the error scales with shock strength in the single-mode example; however, the model underpredicts the error in the broadband example. Let us consider the implications for DNS and LES separately.

The DNS calculations by Larsson (2008) used grids with $k_0h_{2,3} = 2\pi/96$ in the transverse directions, and refined by factors between 2 and 3 (i.e., $k_0h_1 \lesssim 0.033$) in the shock-normal direction near the shock in order to capture the unidirectionally compressed turbulent structures in that region. Since this was DNS, the energy spectrum of the incoming turbulence decayed rapidly at higher wavenumbers. Applying the RDT-model to the actual spectrum in the DNS (rather than Eqn. (2.2)) yields the predicted

errors $\epsilon_{11} \approx 0.9(k_0h)^2$ and $\epsilon_{22} \approx 1.7(k_0h)^2$. This implies errors of less than 0.2% on the DNS grids, and therefore the error induced *at* the shock was not dominant in these calculations. At higher Reynolds numbers, on finer grids, this will be even more true.

The story is different in LES. The RDT-model (with the truncated von Karman spectrum) predicts $\epsilon_{22} \approx 2.6(k_0h)^2$ for the broadband turbulence example presented here. This implies that $k_0h \lesssim 0.062$ is needed for 1% error, or equivalently $k_{\max}/k_0 = \pi/(k_0h) \gtrsim 50$. The transverse grid resolution in LES should be such that $k_{\max}$ is in the early inertial subrange, say $k_{\max}/k_0 \approx 8$ or so (this corresponds to using a 64^3 grid for isotropic turbulence with $k_0 = 4$). Hence the grid must be refined by a factor of 6 in the shock-normal direction to minimize the error at the shock. If the underprediction of the error by the RDT-model in the example presented here is taken into account, an additional factor of 2-3 is needed. This is a very severe restriction on the required grid.

It is not clear, however, that such a strict requirement is necessary in practice. The damping occurs primarily at the smallest resolved scales, so these will be underpredicted on the downstream-side of the shock. If the subgrid model compensates appropriately, either by introducing energy at those scales ("backscatter") or by decreasing the energy transfer for some distance behind the shock, then it is possible that the overall LES results will still be accurate, even in the presence of significant errors at the shock. Therefore, the present work suggests that there is a need to investigate how LES subgrid models behave at and behind a shock, and also that the numerical damping at the shock should be taken into account in such studies. Since different numerics introduce different amounts of damping, it is also clear that any given subgrid model should be tested with different numerical methods for a thorough evaluation.

Finally, we mention the possibility of using the error predictions developed here in grid adaptation algorithms (presumably for unstructured grids). In that case, the predicted error could be used to determine the size and shape of the adapted grid cells near shocks.

Acknowledgments

Financial support has been provided by the DOE SciDAC program (grant DE-FC02-06-ER25787) and NASA (grant NNX08AB30A), with computer time provided through the DOE ERCAP and INCITE programs.

REFERENCES

Jiang, G.-S. & Shu, C.-W. 1996 Efficient implementation of weighted ENO schemes. *J. Comput. Phys.* **126**, 202–228.

Larsson, J. 2008 Direct numerical simulation of canonical shock/turbulence interaction. In *Annual Research Briefs*. Center for Turbulence Research.

Larsson, J., Lele, S. K. & Moin, P. 2007 Effect of numerical dissipation on the predicted spectra for compressible turbulence. In *Annual Research Briefs*, pp. 47–57. Center for Turbulence Research.

Mittal, R. & Moin, P. 1997 Suitability of upwind-biased finite difference schemes for large-eddy simulation of turbulent flows. *AIAA J.* **35** (8), 1415–1417.

Pope, S. B. 2000 *Turbulent Flows*. Cambridge University Press.

Ristorcelli, J. R. & Blaisdell, G. A. 1997 Consistent initial conditions for the DNS of compressible turbulence. *Phys. Fluids* **9** (1), 4–6.